

## **Calcium isotope and Ca/Sr ratios in Douglas Fir (*Pseudotsuga menziesii*) tissues: expectations and reality**

Thomas Bullen<sup>a</sup>, Jenny Dauer<sup>b</sup> and Steven Perakis<sup>c</sup>

<sup>a</sup> U.S. Geological Survey, Water Mission Area (emeritus), Menlo Park, CA 94501 USA (tdbullen@usgs.gov)

<sup>b</sup> School of Natural Resources, University of Nebraska-Lincoln, Nebraska USA

<sup>c</sup> U.S. Geological Survey, Forest and Rangeland Ecosystem Science Center, Corvallis OR 97331 USA

Previous attempts to identify the sources of and biogeochemical cycling pathways of the inorganic nutrient calcium (Ca) in forest ecosystems have relied largely on determining Ca mass fluxes to feeder roots from soil-bedrock and atmospheric sources using chemical (e.g. Ca/Sr ratios), isotopic (e.g. Ca stable isotopes, Sr radiogenic isotopes) and mass balance (e.g. input-output box model) approaches. Until recently little attention has been given to characterizing the chemical and Ca isotope compositions of potential within-tree sources of renewable, resilient Ca such as calcium oxalate ( $\text{CaC}_2\text{O}_4 \cdot (\text{H}_2\text{O})_n$ ) that would be deposited on the forest floor as foliage, twig and bark litter and potentially available for recycling by roots. In this study we focused on characterization of Ca stable isotope ( $\delta^{44/40}\text{Ca}$ ) and Ca/Sr ratios of variously soluble Ca pools including a separate Ca oxalate pool in above ground tissues (foliage, bole wood, xylem, bark) from Douglas fir trees as well as in litter from the underlying forest floor and in soil extracts. Samples described here were collected from a site in the Oregon Coast Range (USA) having relatively high soil Ca-status (high-Ca, low-nitrogen (N)) compared to other sites within a broader study area which displays a spectrum of decreasing Ca status with increasing N status (Perakis and Sinkhorn, 2011).

In several previous studies of Ca isotope systematics of forest ecosystems (e.g. Schmitt et al, 2017 and references therein), Ca oxalate has been invoked as a possible storehouse of isotopically light Ca in tree tissues due largely to analogy to the mineral calcite ( $\text{CaCO}_3$ ) which is characterized by lighter to similar Ca isotope composition compared to coexisting aqueous Ca in a variety of (bio)geochemical environments (e.g. Fantle and Tipper, 2014). On the other hand, theoretical considerations reveal that the hydrated Ca oxalate complex has a significantly greater reduced isotope partition function ( $1000 \ln \beta = 17$  at 25°C) compared to that for hydrated calcium ions ( $1000 \ln \beta = 13-15$  at 25°C depending on hydration coordination), leading Moynier and Fujii (2017) to suggest that  $\delta^{44/40}\text{Ca}$  of Ca oxalate precipitated in tree tissues should be 2-4‰ greater than that of “free Ca” in the transpiration stream. This of course assumes that the Ca oxalate crystals would grow by systematic addition of Ca oxalate complexes rather than individual Ca and oxalate ions from solution to crystal nuclei. These workers further suggested that precipitation of Ca oxalate containing isotopically heavy Ca in foliage could account for the observation that foliage tends to have the heaviest Ca of all tree tissues (e.g. Page et al., 2008; Schmitt et al., 2017). In addition, Ca oxalate has been assumed to have substantially greater Ca/Sr ratios than coexisting fluids due to the greater solubility of Sr oxalate compared to Ca oxalate aqueous complexes (e.g. Handbook of Chemistry and Physics solubility tables). As a starting point for understanding Ca isotope as well as Ca and Sr partitioning between Ca oxalate and coexisting fluids and to provide context for the tree tissue analysis, we performed a Ca-oxalate synthesis experiment under controlled laboratory conditions and compared the results to observed tree tissue compositions.

### **Ca oxalate synthesis experiment: setup and results**

For the Ca oxalate synthesis experiment calcium chloride and sodium oxalate solutions were mixed at 23°C to yield 10 mL of solution with a concentration of 1mM of both calcium and oxalate ion in ten identical serum vials. Following an initial shaking of each vial, samples were allowed to sit until sampling. Samples were poured into a syringe, filtered with 13 mm Whatman Nucleopore polycarbonate Track-etch membranes (0.8  $\mu\text{m}$ ) to separate solid Ca oxalate crystals, and syringe filters were rinsed 2 times with 3 mL of Nanopure water. After the initial sampling at  $t = 0$  minutes, repeat sampling occurred at 5, 10, 20, 40, 60, 120, 360, 1440, and 2880 minutes. Filters were cut in half for chemical and isotopic analysis, and for crystal inspection. Solutions were acidified with 0.5 mL 12 N HCl. Both the solutions and half-filters were analyzed at U. S. Geological Survey in Menlo Park, CA for Ca and Sr concentrations by inductively-coupled plasma mass spectrometry (ICPMS), and for  $^{44}\text{Ca}/^{40}\text{Ca}$  isotope ratios by thermal-ionization mass spectrometry (TIMS) using a “double spike” approach (e.g., Perakis et al., 2006; Page et al., 2008 for analysis of tree and soil samples). Scanning transmission electron microscope (STEM) images of the remaining half filters were taken to track crystal formation using a Philips CM-12 microscope.

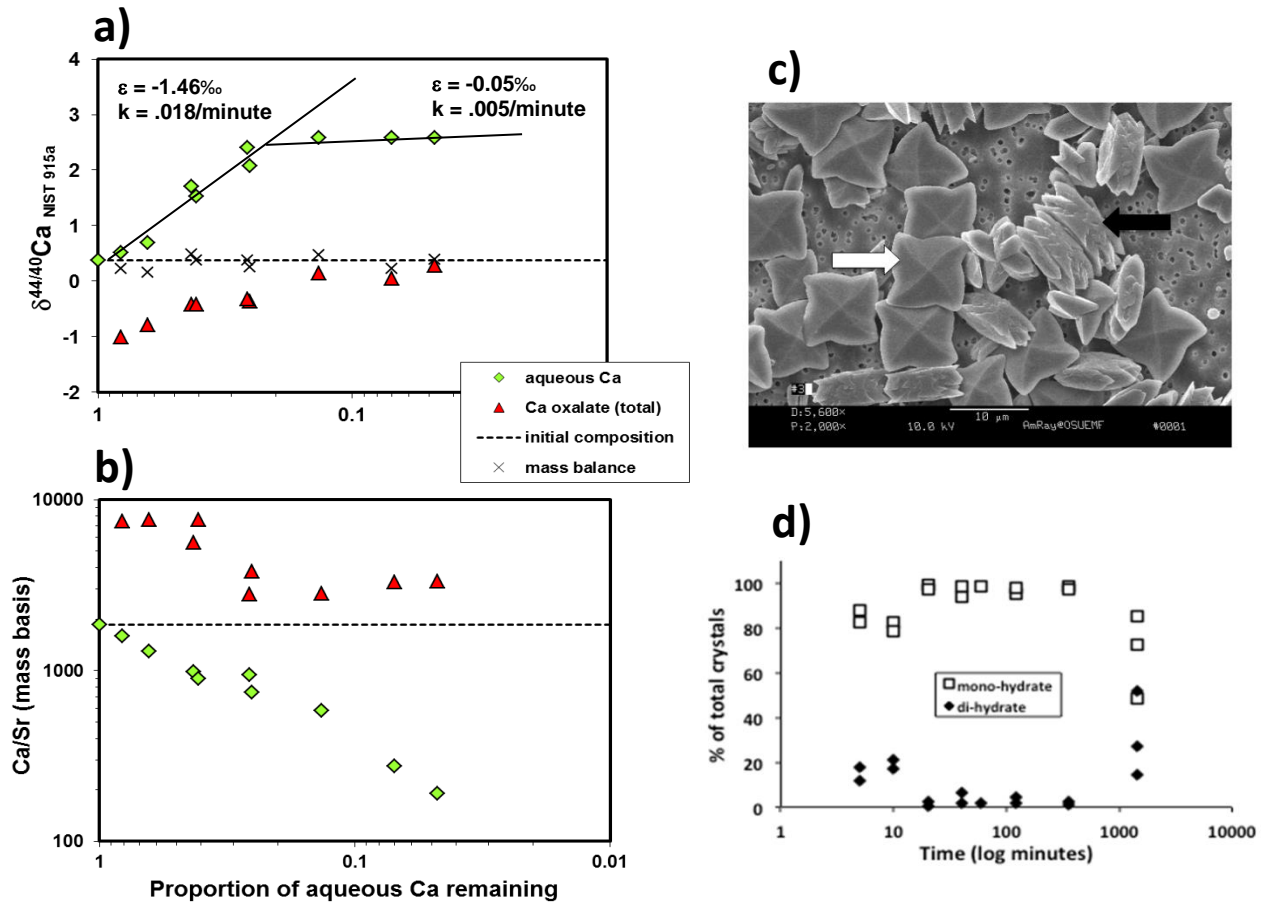


**Figure 1:** a) Ca isotope compositions of total accumulated Ca oxalate and remaining aqueous Ca vs. proportion of aqueous Ca remaining ( $f$ ) over a 48 hour time series. Calculated isotope mass balance at each sampling point is shown relative to the initial Ca isotope composition of the liquid. Crystallization proceeded along two distinct segments noted as a break in the composition trends.  $\epsilon$  is the fractionation factor between Ca oxalate and remaining aqueous Ca for each segment,  $k$  is the rate constant for a second-order reaction. Reproducibility of sample measurements lies within the symbol in all cases. b) Ca/Sr ratios of total accumulated Ca oxalate and remaining aqueous Ca over the time series. c) STEM image of Ca oxalate crystals sampled at  $t=10$  minutes. White arrow points to Ca Oxalate dihydrate (druse form) and black arrow points to Ca oxalate monohydrate (raphide form). d) Visual estimate of proportions of Ca oxalate monohydrate and dehydrate crystals on filters at each sampling time.

Results of the Ca oxalate synthesis experiment are shown in Figure 1. Crystallization proceeded in two stages marked by a significant break in both the Ca isotope and Ca/Sr distribution patterns as a function of proportion of aqueous Ca remaining (Figure 1a). From the initiation of crystallization to about 120 minutes, the apparent fractionation factor  $\epsilon$  between Ca oxalate crystals and dissolved Ca was approximately  $-1.50\text{‰}$  and  $k$ , the rate constant derived from the equation  $df/dt=kf^2$  for a second-order reaction was  $0.018/\text{minute}$ . From the 120 minute time point to the end of the experiment,  $\epsilon$  shifted abruptly to approximately  $0\text{‰}$ , indicating no Ca isotope fractionation between Ca oxalate and dissolved Ca during this portion of the experiment, and  $k$  decreased to  $0.005/\text{minute}$ . Throughout the experiment, Ca/Sr of Ca oxalate was substantially greater than that of the remaining liquid, although Sr incorporation into the Ca oxalate crystals decreased sufficiently with decreasing crystallization rate to reverse the approach of Ca/Sr of the bulk accumulated crystals to that of the starting solution (Figure 1b). Interestingly while Ca oxalate monohydrate crystals were dominant throughout the experiment, Ca oxalate dihydrate crystals were observed in significant proportions only in the very early and final samples taken (Figures 1c, 1d).

The important conclusions are that under the experimental conditions: 1) Ca oxalate had lesser to similar  $\delta^{44/40}\text{Ca}$  to the host solution ( $\Delta^{44/40}\text{Ca}_{\text{Ca-oxalate} - \text{solution}} = -1.5$  to  $0\text{‰}$ ) with fractionation decreasing with decreasing crystallization

rate. There was no evidence of crystals having greater  $\delta^{44/40}\text{Ca}$  than aqueous Ca as suggested by Moynier and Fujii (2017); and 2) Ca oxalate had greater Ca/Sr than the host solution with Sr incorporation into the Ca-oxalate lattice decreasing with decreasing crystallization rate.

## Sequential extraction of Ca from above-ground Douglas fir tissues and soils

This study focused on the chemical and isotopic characterization of above-ground Douglas fir tissues as the primary source of forest floor litter that would be available on a renewable basis for Ca recycling. Multiple foliar age classes and dead needles as needle litterfall were collected to represent a time continuum of needle aging. In 2007, sun needles and needle-litterfall were collected from three trees at the end of the growing season (Sept/Oct). Live foliage was separated into 5 age classes, and needle-litterfall was collected without age-class separation. In May 2010 three trees were cored twice with an increment borer and separated into bark and bole-wood (sap-wood only) tissues. Four additional bark samples were taken with a 2 cm diameter x 2 cm deep corer. To separately analyze phloem chemistry, the inner-bark with moist, light-colored tissues approximately 2 mm deep was removed from the rest of the bark. Samples were composited into a single sample of inner-bark, outer-bark and bole-wood. Live and dead needles, inner-bark, outer-bark and bole-wood samples were flash frozen in an 80°C cooler and subsequently freeze-dried (Virtis 35L Genesis Super XL, SP Industries, Warminster, PA, USA). The Douglas fir tissues were subjected to a three-stage dissolution process using progressively aggressive digest media that separated operational Ca fractions that we interpret to represent water soluble free-Ca, pectate- and lignin-bound “structural” Ca (acetic acid soluble) and Ca-oxalate (HCl soluble) in order of increasing resistance to dissolution (Dauer and Perakis, 2014).

Soils underlying the sampled trees were collected in June 2010 by removing and retaining the forest floor layer, sampling 0-10 cm deep with a 5.1 cm diameter soil corer, followed by 10-20 cm and 70-100 cm deep with an 4 cm diameter slide hammer. Soils were sieved to 2 mm to remove rocks and debris and to homogenize the soil, composited and air-dried at room temperature. These soils received a sequential treatment, yielding exchangeable and leachable fractions (Bullen and Bailey, 2005; Perakis et al., 2006). The exchangeable fraction was assayed by equilibrating 5 g of soil with 50 mL of 0.1 N  $\text{NH}_4\text{OAc}$  for 24 h. The leachable fraction was assayed by thoroughly rinsing 1 g of soil remaining from the exchange procedure with de-ionized water and combining with 10 mL of 1 N  $\text{HNO}_3$  for 24 h at 30° C. Following filtration sample solutions were analyzed for Ca and Sr concentrations and  $\delta^{44/40}\text{Ca}$  using techniques similar to those described above for the Ca oxalate synthesis experiment.

Results of the tree tissue and soil sequential extractions are shown in Figure 2. For foliage and litter,  $\delta^{44/40}\text{Ca}$  generally decreased with increasing pool recalcitrance such that the Ca-oxalate fraction contained the lightest Ca. Across foliar age classes, the difference in  $\delta^{44/40}\text{Ca}$  between Ca oxalate and soluble fractions ( $\Delta^{44/40}\text{Ca}_{\text{Ca oxalate-soluble}}$ ) averaged -1.03‰, ranging from -0.51 to -1.47‰. On the other hand, in bolewood the three operational fractions had essentially identical  $\delta^{44/40}\text{Ca}$  values; in bark the water soluble and Ca oxalate fractions had essentially identical and low  $\delta^{44/40}\text{Ca}$  values while “structural” Ca constituted a pool of heavier Ca. Thus for the tissues overall,  $\Delta^{44/40}\text{Ca}_{\text{Ca oxalate-soluble}}$  ranged from -1.47 to 0‰ consistent with the results of the Ca oxalate synthesis experiment. For foliage and litter, Ca/Sr ratios were greater in the Ca-oxalate fraction compared to values in the other fractions. This contrasts with results for the wood components in which Ca/Sr values decreased systematically with increasing pool recalcitrance such that Ca/Sr ratios were least in the Ca oxalate fraction at odds with the results of the Ca oxalate synthesis experiment. An intriguing feature of the data is the persistent increase of Ca/Sr ratio of the Ca oxalate fraction of the foliage with increasing needle age class. The increase of Ca/Sr ratio in the foliage samples across age classes corresponds to a 6-fold increase in Ca concentration and 3-fold increase in Sr concentration in the Ca oxalate fraction, with little change of Ca or Sr concentrations in the soluble and structural Ca fractions. This indicates that Ca oxalate continues to precipitate in the foliage as it ages on the stem which will greatly influence litter composition. While the experimental results are thus both consistent with and at odds with the tissue analysis, they provide a basis for evaluating physiological factors that influence Ca isotope and Ca/Sr allocation along transpiration pathways within trees (e.g., formation of bark with Ca oxalate having light Ca and low Ca/Sr provides a convenient mechanism to create transpiring fluids having heavy Ca and high Ca/Sr destined for the canopy).

The exchangeable and acid extractable fractions of the soils displayed similar  $\delta^{44/40}\text{Ca}$  and Ca/Sr distributions with depth.  $\delta^{44/40}\text{Ca}$  values of both fractions generally increased with depth, with forest floor extracts containing the lightest Ca. Ca/Sr values of extracts generally decreased with depth, with forest floor extracts having the greatest Ca/Sr values. The forest floor Ca isotope composition of the extracts apparently requires some combination of dead needle and bark components while the compositions of deeper extracts tend toward the composition of bedrock, suggesting a broad mixing relationship.

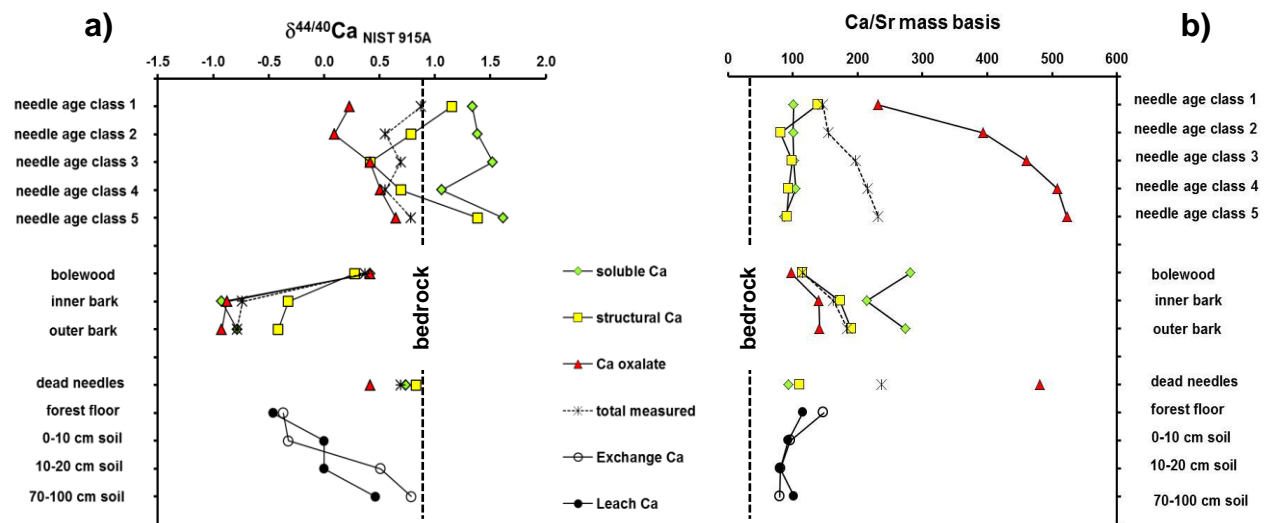


**Figure 2:** Ca isotope compositions (a) and Ca/Sr ratios (b) of Douglas fir tissue and soil sequential extractions. Line labeled “bedrock” represents the average  $\delta^{44/40}\text{Ca}$  and Ca/Sr compositions of total digestions of 3 sandstone blocks pulled from soil sample bags and 5 soil samples, all of which had remarkably similar  $\delta^{44/40}\text{Ca}$  values and Ca/Sr ratios. In each figure, total measured compositions compare well with summed compositions of individual fractions (not shown to aid clarity of figures).

## A simple catchment-scale perspective

Based on these results we suggest that forest floor litter (mainly foliage with branches and bark shed from the trunk), which constitutes an important potential source of Ca nutrition for trees, is likely to consist of at least two distinct Ca pools that may be subject to different fates: 1) one having relatively heavy Ca and low Ca/Sr ratio that is easily dissolved by precipitation and weakly acidic solutions with Ca prone to downward transfer to soil exchange sites where it might be available as plant nutrition via biolifting or captured by drainage waters; and 2) one having relatively light Ca and high Ca/Sr ratio (as Ca-oxalate crystals) that would be relatively insoluble and thus reside in shallow organic soils with Ca available for consumption through the strong-acid action of mycorrhizal symbionts associated with fine feeder roots of trees or microbial activity.

## References

- Bullen, T.D. and Bailey, S.W. (2005) Identifying calcium sources at an acid deposition-impacted spruce forest: a strontium isotope, alkaline earth element multi-tracer approach. *Biogeochemistry*, 74: 63–99.
- Dauer, J.M. and Perakis, S.S. (2014) Calcium oxalate contribution to calcium cycling in forests of contrasting nutrient status. *Forest Ecology Management*, 334: 64–73.
- Fantle, M.S. and Tipper, E.T. (2014) Calcium isotopes in the global biogeochemical Ca cycle: Implications for development of a Ca isotope proxy. *Earth-Science Reviews*, 129:148–177
- Moynier, F. and Fujii, T. (2017) Calcium isotope fractionation between aqueous compounds relevant to low-temperature geochemistry, biology and medicine. *Sci. Rep. Nature*, 7: 44255/doi: 10.1038/srep44255.
- Perakis, S.S., Maguire, D.A., Bullen, T.D., Cromack, K., Waring, R.H. and Boyle, J.R. (2006) Coupled nitrogen and calcium cycles in forests of the Oregon Coast Range. *Ecosystems*, 9: 63–74.
- Page, B.D., Bullen, T.D. and Mitchell, M.J. (2008) Influences of calcium availability and tree species on Ca isotope fractionation in soil and vegetation. *Biogeochemistry*, 88: 1–13.
- Perakis, S., Sinkhorn, E. (2011) Biogeochemistry of a temperate forest nitrogen gradient. *Ecology*, 92: 1481–1491.
- Schmitt, A.D., Gangloff, S., Labolle, F., Chabaux, F., Stille, P. (2017) Calcium biogeochemical cycle at the beech tree-soil interface from the Strengbach CZO (NE France): insights from stable Ca and radiogenic Sr isotopes. *Geochimica et Cosmochimica Acta*, 213: 91–109.